

Optimization of a Pb²⁺-Directed Gold Nanoparticle/DNAzyme Assembly and Its Application as a Colorimetric Biosensor for Pb²⁺

Juewen Liu and Yi Lu*

Department of Chemistry, University of Illinois at Urbana-Champaign, Urbana, Illinois 61801

Received April 1, 2004. Revised Manuscript Received May 27, 2004

We previously communicated a method for directed assembly of gold nanoparticles using a Pb²⁺-dependent DNAzyme and demonstrated the application of this system as a colorimetric biosensor. The sensor shows high sensitivity and selectivity toward Pb²⁺ and undergoes a blue-to-red color transition in the presence of Pb²⁺. To gain a deeper insight into the analyte-directed nanomaterials assembly and sensing processes, a detailed characterization of the system has been performed. First, we found that the presence of gold nanoparticles had no effect on the Pb²⁺-dependent activity of the DNAzyme and the presence of DNAzyme had little effect on the melting properties of the DNA-functionalized nanoparticle aggregates, suggesting that the performance of the nanoparticle and DNAzyme systems can be optimized independently. Second, the optimal length of the DNAzyme and the alignment of the DNA-functionalized gold nanoparticles for the assembly and sensing processes have been determined to be 9 base pairs on each end for the DNAzyme, and “head-to-tail” alignment for the DNA-functionalized gold nanoparticles. Third, the optimal stoichiometry of the enzyme to the substrate strands of the DNAzyme was shown to be one to one in nanoparticle aggregates. Finally, the most favorable temperature and pH conditions for the system have also been established, with a temperature of 37 °C and pH of 6.4 to 9.2 as the best operating conditions. The study also revealed that, for most efficient assembly of nanoparticles, the DNA backbone should be rigidified by formation of a double helix with other DNA molecules. These findings allow optimization of the processes for directed assembly of nanomaterials and for colorimetric sensing.

Introduction

The directed assembly of nanomaterials using DNA as a template has received more and more attention recently, largely because of the predictable structure and the ease of chemical synthesis, modification, and assembly of DNA molecules.^{1–6} This endeavor has resulted in new materials with novel structures and properties.^{1,5,7,8} One remarkable example is the control of the optical properties of oligonucleotide-functionalized gold nanoparticles with DNA.¹ In the presence of complementary DNA strands, nanoparticles can assemble because of DNA base-pairing interactions, giving rise to a red-to-blue color transition. This property has been utilized to design highly sensitive and selective colorimetric biosensors for DNA detection.^{9,10} The design is

based on not only the structural properties of DNA molecules but also the function of DNA to recognize complementary DNA.

In addition to the recognition of complementary DNA as a means for genetic information storage, DNA has recently been found to carry out catalytic functions,^{11–13} including DNA/RNA cleavage,^{14,15} ligation,^{16,17} phosphorylation,¹⁸ and porphyrin metalation.¹⁹ These catalytic DNA molecules are known as DNAzymes. Of particular interest are RNA-cleaving DNAzymes, because they can be conveniently isolated using a combinatorial biology approach called *in vitro* selection.^{11,12,20} More importantly, many of the DNAzymes have shown

* To whom correspondence should be addressed. Tel: (217) 333-2619. Fax: (217) 333-2685. E-mail: yi-lu@uiuc.edu.

- (1) Mirkin, C. A.; Letsinger, R. L.; Mucic, R. C.; Storhoff, J. J. *Nature* **1996**, *382*, 607–609.
- (2) Alivisatos, A. P.; Johnsson, K. P.; Peng, X.; Wilson, T. E.; Loweth, C. J.; Bruchez, M. P., Jr.; Schultz, P. G. *Nature* **1996**, *382*, 609–611.
- (3) Niemeyer, C. M. *Angew. Chem., Int. Ed.* **2001**, *40*, 4128–4158.
- (4) Seeman, N. C. *Nature* **2003**, *421*, 427–431.
- (5) Yan, H.; Park, S. H.; Finkelstein, G.; Reif, J. H.; LaBean, T. H. *Science* **2003**, *301*, 1882–1884.
- (6) Shih, W. M.; Quispe, J. D.; Joyce, G. F. *Nature* **2004**, *427*, 618–621.
- (7) Yan, H.; Zhang, X.; Shen, Z.; Seeman, N. C. *Nature* **2002**, *415*, 62–65.
- (8) Li, J. J.; Tan, W. *Nano Lett.* **2002**, *2*, 315–318.

- (9) Elghanian, R.; Storhoff, J. J.; Mucic, R. C.; Letsinger, R. L.; Mirkin, C. A. *Science* **1997**, *277*, 1078–1080.

- (10) Storhoff, J. J.; Elghanian, R.; Mucic, R. C.; Mirkin, C. A.; Letsinger, R. L. *J. Am. Chem. Soc.* **1998**, *120*, 1959–1964.

- (11) Breaker, R. R. *Nat. Biotechnol.* **1997**, *15*, 427–431.
- (12) Sen, D.; Geyer, C. R. *Curr. Opin. Chem. Biol.* **1998**, *2*, 680–687.

- (13) Lu, Y. *Chem. Eur. J.* **2002**, *8*, 4588–4596.
- (14) Santoro, S. W.; Joyce, G. F. *Proc. Natl. Acad. Sci. U.S.A.* **1997**, *94*, 4262–4266.

- (15) Carmi, N.; Shultz, L. A.; Breaker, R. R. *Chem. Biol.* **1996**, *3*, 1039–1046.

- (16) Cuenoud, B.; Szostak, J. W. *Nature* **1995**, *375*, 611–614.

- (17) Coppins, R. L.; Silverman, S. K. *Nat. Struct. Mol. Biol.* **2004**, *11*, 270–274.

- (18) Li, Y.; Breaker, R. R. *Proc. Natl. Acad. Sci. U.S.A.* **1999**, *96*, 2746–2751.

- (19) Li, Y.; Sen, D. *Nat. Struct. Biol.* **1996**, *3*, 743–747.
- (20) Breaker, R. R.; Joyce, G. F. *Chem. Biol.* **1994**, *1*, 223–229.

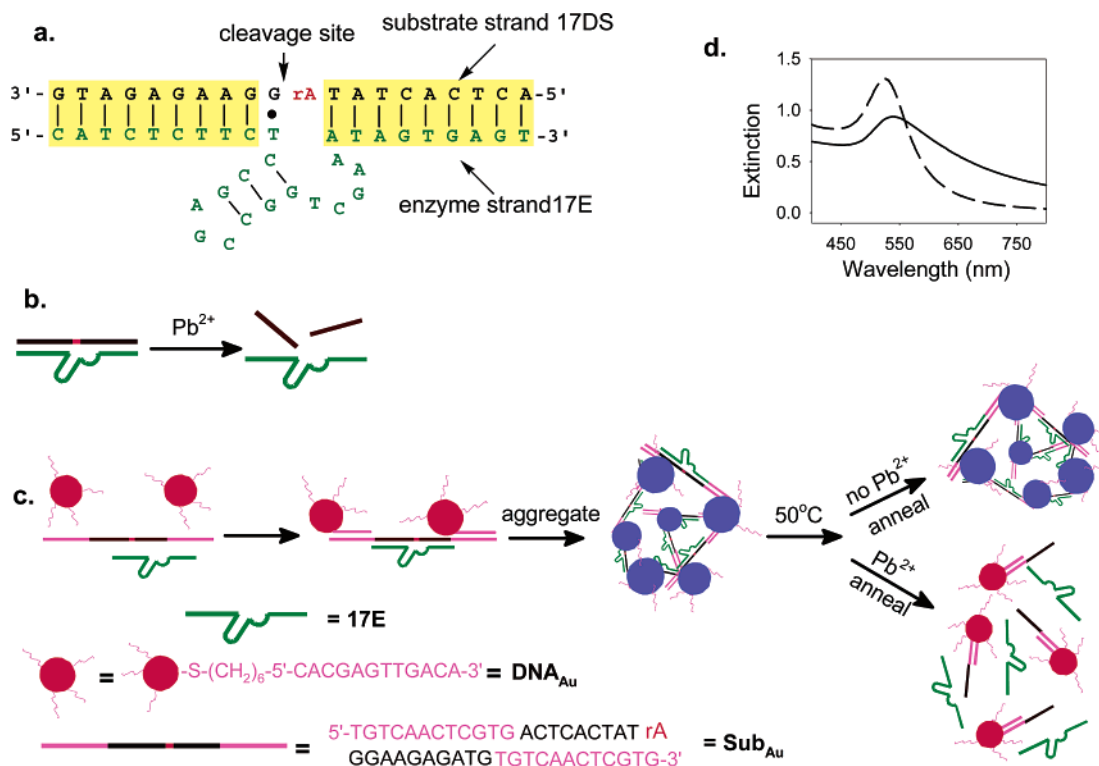


Figure 1. (a) Secondary structure of the "8-17" DNzyme system that consists of an enzyme strand (17E) and a substrate strand (17DS). The cleavage site is indicated by a black arrow. Except for a ribonucleoside adenosine at the cleavage site (rA), all other nucleosides are deoxyribonucleosides. The two yellow boxes indicate the substrate binding regions of the DNzyme. (b) Cleavage of 17DS by 17E in the presence of Pb²⁺. (c) Schematic illustration of DNzyme-directed assembly of gold nanoparticles and their application as colorimetric biosensors for metal ions such as Pb²⁺. In this system, 17DS has been extended on both the 3' and 5' ends by 12 bases, which are complementary to the 12-mer DNA attached to the 13-nm gold nanoparticles (DNA_{Au}). (d) UV-vis extinction spectra of the sensor in the absence (solid curve) or presence (dashed curve) of 5 μM Pb²⁺. The Pb²⁺-activated cleavage results in separated nanoparticles.

metal-dependent activities, and can therefore be used to design metal sensors. For example, DNzymes that are highly specific toward Pb²⁺,²⁰ Zn²⁺,²¹ and Co²⁺²² have been obtained. To transform the metal-specific activity of DNzymes into physically detectable signals, fluorophore-labeling has been used.²²⁻²⁴ Another equally attractive and perhaps even simpler method is colorimetric detection, because for qualitative or semiquantitative analysis it can eliminate the need for use of an analytical instrument and can therefore make on-site, real-time, detection and quantification easier.

Inspired by the success of the nanoparticle-based colorimetric sensors for DNA detection,^{9,10} we employed a Pb²⁺-dependent DNzyme to assemble nanoparticles and demonstrated that the nanoparticles showed different assembly states controlled by the concentration of Pb²⁺ in the system.²⁵ Highly sensitive and selective colorimetric Pb²⁺ sensors have been designed on the basis of this phenomenon.²⁵ The DNzyme used for the sensor is known as the "8-17" DNzyme (Figure 1a), which has been isolated under several different *in vitro* selection conditions,^{14,26,27} and shows very high activity in the presence of Pb²⁺.²⁸ The DNzyme is composed

of a substrate strand (17DS) and an enzyme strand (17E). The substrate strand is a DNA/RNA chimer with a single RNA linkage (ribonucleoside adenosine, rA) that serves as the cleavage site (Figure 1a). In the presence of Pb²⁺, the substrate is cleaved into two pieces by the enzyme (Figure 1b).

Because of the toxicity of Pb²⁺,²⁹ sensors for simple Pb²⁺ detection and quantification are highly desirable.^{23,30-33} To engineer the Pb²⁺-dependent DNzyme into a colorimetric biosensor, gold nanoparticles (13 nm diameter) functionalized with 5'-thiol-modified 12-mer DNA (named DNA_{Au}) were used as color reporting groups. The original substrate strand (17DS) was extended on both ends for 12 bases. The extended substrate is called Sub_{Au}, which can hybridize to a DNA_{Au} on each end. Therefore, through DNA base-pairing interactions, the enzyme (17E), the extended substrate (Sub_{Au}), and DNA_{Au} can assemble to form

(26) Faulhammer, D.; Famulok, M. *Angew. Chem., Int. Ed. Engl.* **1996**, *35*, 2837-2841.

(27) Li, J.; Zheng, W.; Kwon, A. H.; Lu, Y. *Nucleic Acids Res.* **2000**, *28*, 481-488.

(28) Brown, A. K.; Li, J.; Pavot, C. M. B.; Lu, Y. *Biochemistry* **2003**, *42*, 7152-7161.

(29) Needleman, H. L. *Human Lead Exposure*; CRC Press: Boca Raton, FL, 1992.

(30) Teltting-Diaz, M.; Bakker, E. *Anal. Chem.* **2002**, *74*, 5251-5256.

(31) Chen, C.-T.; Huang, W.-P. *J. Am. Chem. Soc.* **2002**, *124*, 6246-6247.

(32) Blake, D. A.; Jones, R. M.; Blake, R. C.; Pavlov, A. R.; Darwish, I. A.; Yu, H. *Biosens. Bioelectron.* **2001**, *16*, 799-809.

(33) Deo, S.; Godwin, H. A. *J. Am. Chem. Soc.* **2000**, *122*, 174-175.

(21) Santoro, S. W.; Joyce, G. F.; Sakthivel, K.; Gramatikova, S.; Barbas, C. F., III. *J. Am. Chem. Soc.* **2000**, *122*, 2433-2439.

(22) Mei, S. H. J.; Liu, Z.; Brennan, J. D.; Li, Y. *J. Am. Chem. Soc.* **2003**, *125*, 412-420.

(23) Li, J.; Lu, Y. *J. Am. Chem. Soc.* **2000**, *122*, 10466-10467.

(24) Liu, J.; Lu, Y. *Anal. Chem.* **2003**, *75*, 6666-6672.

(25) Liu, J.; Lu, Y. *J. Am. Chem. Soc.* **2003**, *125*, 6642-6643.

blue-colored nanoparticle aggregates as shown in Figure 1c.^{1,9,25} Although only the substrate strand is acting as the linker, the presence of the enzyme is required for the formation of the aggregates (vide infra). These blue aggregates can be isolated and used as colorimetric sensors for Pb^{2+} . If the aggregates are heated to above 50 °C ($T_m = 46$ °C), and allowed to cool slowly to room temperature in the presence of Pb^{2+} , Sub_{Au} is cleaved by the enzyme in the cooling process. Because cleaved Sub_{Au} can no longer assemble nanoparticles, a red color due to separated nanoparticles will be observed. However, if no Pb^{2+} is present, nanoparticles, 17E, and Sub_{Au} will re-assemble and show a blue color. The colors can be conveniently observed by spotting the resulting sensor solution onto a TLC plate. The sensor is highly sensitive and selective for Pb^{2+} . Using UV-vis spectroscopy, Pb^{2+} can be quantified in a range from 100 nM to 4 μM .²⁵ The Pb^{2+} detection range for this sensor can be tuned over several orders of magnitude by introducing an inactive variant of the DNAzyme. This important characteristic allows accurate determination of Pb^{2+} concentration without signal saturation.²⁵

By using DNAzymes specific for other metal ions, the DNAzyme-nanoparticle-based detection method could be applied to design of colorimetric sensors for other metal ions. Recently, we have extended the range of analytes that can be detected by using this method beyond metal ions to analytes such as adenosine³⁴ by introducing aptamers into the above DNAzyme system to form aptazymes (allosteric DNAzymes).^{35–39} Therefore, it is important to further understand the properties of the new biomaterial system for better sensor design. In this paper, we report a full characterization and optimization of the DNAzyme-nanoparticle system, including the effect of nanoparticles on the DNAzyme activity, the DNAzyme sequence optimization, the melting properties and stoichiometry of the system, and the effects of temperature and pH on the Pb^{2+} -directed assembly of nanoparticles.

Results and Discussion

Effects of Gold Nanoparticles on the DNAzyme Activity. One concern about the use of gold nanoparticles to signal the DNAzyme activity is that nanoparticles might interfere with the metal-dependent activities of the DNAzyme, for example, by DNAzymes or Pb^{2+} absorbing onto nanoparticle surfaces. To investigate whether the DNAzyme maintains the same activity in the presence of DNA-functionalized gold nanoparticles, a biochemical assay was performed.^{14,26,27} The DNAzyme cleavage kinetics curves in the presence (open triangles) and absence (dots) of gold nanoparticles are presented in Figure 2. The two curves overlapped very well, indicating that the DNAzyme cleaved its substrate with the same efficiency, regardless of whether

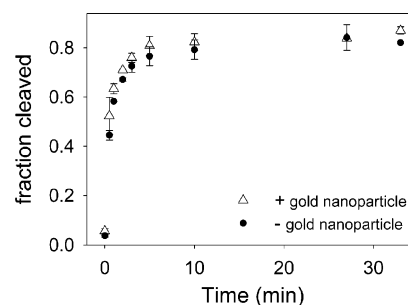


Figure 2. DNAzyme activity assay in the presence (triangles) and absence (dots) of 12-mer DNA-functionalized gold nanoparticles (DNA_{Au}). The excellent overlap of the two reaction kinetics curves indicates the minimal effect of nanoparticles on the activities of DNAzymes.

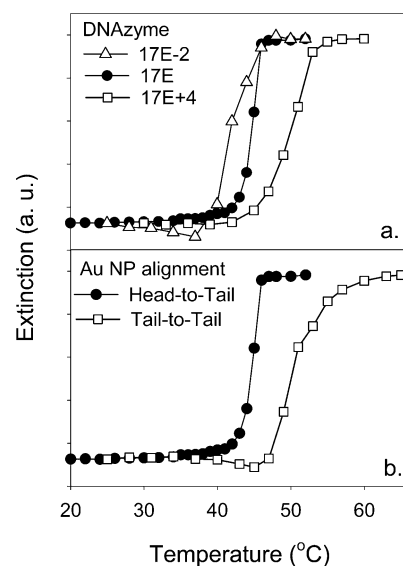


Figure 3. Melting properties of DNAzyme-assembled gold nanoparticles (Au NP). (a) melting curves of nanoparticles assembled by DNAzymes of different lengths, and (b) melting curves of nanoparticles with different alignments. Extinctions are normalized for comparison.

the gold nanoparticles were present or not. This result indicates that the DNAzyme and gold nanoparticles are fully compatible and the performance of the nanoparticle and the DNAzyme systems can be optimized separately.

Optical Properties of DNAzyme-Assembled Nanoparticles. Similar to gold nanoparticles assembled by complementary DNA, nanoparticles assembled by DNAzymes also show strong distance-dependent optical properties, which is the basis for the colorimetric detection. Separated 13-nm-diameter gold nanoparticles have a surface plasmon peak at 522 nm (Figure 1d, dashed curve), giving the intense red color to the nanoparticles. After the DNAzyme-induced assembly, the 522-nm peak decreases in intensity and shifts to longer wavelength, resulting in an increase of the extinction in the 700-nm region (Figure 1d, solid curve), and a blue color. Therefore, the extinction ratio at 522 and 700 nm has been used to monitor the aggregation state of nanoparticles. A higher ratio is associated with a red color of separated nanoparticles, while a lower ratio is associated with a blue color of aggregated nanoparticles. Compared to monitoring other properties, such as the melting temperature of nanoparticle ag-

(34) Liu, J.; Lu, Y. *Anal. Chem.* **2004**, *76*, 1627–1632.

(35) Ellington, A. D.; Szostak, J. W. *Nature* **1992**, *355*, 850–852.

(36) Wilson, D. S.; Szostak, J. W. *Annu. Rev. Biochem.* **1999**, *68*, 611–647.

(37) Jayasena, S. D. *Clin. Chem.* **1999**, *45*, 1628–1650.

(38) Seetharaman, S.; Zivarts, M.; Sudarsan, N.; Breaker, R. R. *Nat. Biotechnol.* **2001**, *19*, 336–341.

(39) Wang, D. Y.; Lai, B. H. Y.; Sen, D. *J. Mol. Biol.* **2002**, *318*, 33–43.

Table 1. Names and Sequences of DNA Used in the Paper

name	sequence (from 5'-end to 3'-end)
17E	CATCTCTTCTCCGAGCCGGTCCGAAATAGTGAGT
17E-2	ATCTCTTCTCCGAGCCGGTCCGAAATAGTGAG
17E+4	GACATCTCTTCTCCGAGCCGGTCCGAAATAGTGAGTTG
Sub _{Au}	TGCAACTCGTGACTCACTATrAGGAAGAGATGTGTCAACTCGTG
Sub _{Au} -2	GTCAACTCGTGACTCACTATrAGGAAGAGATGTGTCAACTCGTG
Sub _{Au} +4	CATGTCAACTCGTGACTCACTATrAGGAAGAGATGTGTCAACTCGTGT
35Sub _{Au}	CATCTGTGAACACTCACTATrAGGAAGAGATGTGTCAACTCGTG
DNA _{Au}	Au nanoparticle-S-(CH ₂) ₆ -CACGAGTTGACA
3DNA _{Au}	TCACAGATGAGT-(CH ₂) ₃ -S-Au nanoparticle
Anti-17DS	CATCTCTTCTATAGTGAGT

gregates,⁴⁰ the ratiometric method allows simple and fast quantification with minimal effects from sampling conditions.

Melting Properties of DNAzyme-Assembled Nanoparticles. DNA-assembled gold nanoparticles have melting properties characterized by the sharp melting transition,^{9,10} suggesting a cooperative mechanism.⁴⁰ To compare the physical properties of gold nanoparticles assembled by complementary DNA and by DNAzymes, we studied the melting properties of DNAzyme-assembled nanoparticles, and found that the DNAzyme-assembled nanoparticles showed similarly sharp melting transitions. The melting curves were obtained by monitoring the extinction at 260 nm with temperature increase (Figure 3). For a better comparison of the two systems, the length of the DNAzyme and the alignment of nanoparticles were varied. The DNAzyme has two substrate binding regions (Figure 1a, yellow boxes) and a catalytic core. The length of the substrate binding region can be varied without significant changing of the catalytic properties of the DNAzyme, as long as the catalytic core is maintained.^{28,41} We first extended the substrate binding regions for two base pairs on both ends. The resulting extended enzyme strand is named 17E+4, and the corresponding substrate is named Sub_{Au}+4. All DNA sequences are listed in Table 1. The melting temperature of nanoparticle aggregates assembled by the extended DNAzyme is 50 °C (Figure 3a, squares), which is 4 °C higher than nanoparticles assembled by 17E and Sub_{Au} (Figure 3a, circles). If one base pair is deleted from each end of the substrate binding regions, the resulting shortened enzyme is named 17E-2, and the corresponding substrate is named Sub_{Au}-2. The melting temperature drops to 40 °C for the shortened DNAzyme (Figure 3a, triangles). Therefore, longer DNAzymes give higher thermal stability for the nanoparticle aggregates. The reason for the enzyme-dependent melting behavior could be explained as follows. For DNA-assembled nanoparticle systems reported by Mirkin and co-workers, a single base insertion in the linking DNA could decrease the melting temperature by 2.8 °C, which was attributed to the elimination of base-stacking interactions.¹⁰ Removal of an enzyme strand from the aggregate would result in an 18- to 24-base insertion, which could decrease the melting temperature of the aggregates in a similar way.⁴⁰

The effects of changing nanoparticle alignment on the melting temperature were also studied. Using the same

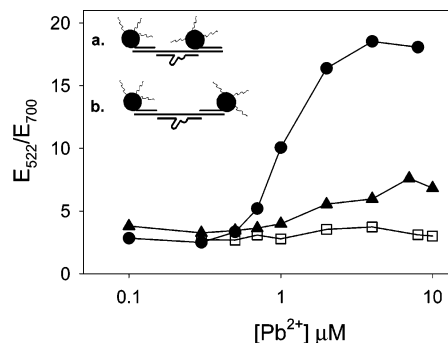


Figure 4. Effect of the DNAzyme length or the nanoparticle alignment on the sensitivity of the sensors. The Pb²⁺ detection curves using 17E and Sub_{Au} (solid circles), and using 17E+4 and Sub_{Au}+4 are shown (solid triangles). For these two curves, the nanoparticles are aligned in the “head-to-tail” manner (inset a). The Pb²⁺ detection curve using 17E and Sub_{Au} but with the “tail-to-tail” alignment (inset b) is also shown (empty squares).

17E enzyme, by changing the substrate sequence from Sub_{Au} to 35Sub_{Au}, and using a mixture of DNA_{Au} and 3DNA_{Au} (see Table 1), the nanoparticle alignment changed from “head-to-tail” to “tail-to-tail” (see inset of Figure 4). The melting temperature increased by 5 °C with this modification, which is consistent with the result reported by Mirkin and co-workers for the nanoparticle aggregates assembled by complementary DNA.⁴⁰

Effects of DNA Length on Nanoparticle Assembly and Pb²⁺ Sensing. To use the DNAzyme-assembled nanoparticles as colorimetric sensors for Pb²⁺ detection, the nanoparticles should show different assembly states directed by Pb²⁺. To obtain the largest difference in nanoparticle assembly state induced by the same Pb²⁺ concentration difference, DNAzymes of different lengths were studied. With the longer DNAzyme (17E+4 and Sub_{Au}+4), the extinction ratio at 522 and 700 nm saturates at ~7 in the presence of Pb²⁺ (Figure 4, solid triangles), as compared to ~18 for the sensor using 17E and Sub_{Au} (Figure 4, solid circles). Therefore, the performance of the sensor is decreased by this modification.

The decreased sensitivity may be due to inhibition of release of the cleaved substrate, allowing the cleaved substrates linked by the enzyme strand to assemble nanoparticles even if they are cleaved. After cleavage, the 48-mer substrate (Sub_{Au}+4) is cut into two smaller pieces of DNA with 24 bases for each piece. Twelve of the 24 bases anneal to the DNA on gold nanoparticles to form a stable structure. For the remaining 12 bases, 11 of them are annealed with the enzyme. This construct should also be stable under experimental conditions, because the difference is only one base pair.

(40) Jin, R.; Wu, G.; Li, Z.; Mirkin, C. A.; Schatz, G. C. *J. Am. Chem. Soc.* **2003**, *125*, 1643–1654.

(41) Santoro, S. W.; Joyce, G. F. *Biochemistry* **1998**, *37*, 13330–13342.

Indeed, after 6 h of incubation at room temperature, the extinction ratios of all samples drop to the baseline level for the 17E+4 DNAzyme system. For the original 17E system (Figure 1A), there are only 9 bases for the cleaved substrate to anneal with the enzyme strand, and the stability of this complex is relatively lower.

Because the extension of the substrate and the enzyme strand decreases the performance of the sensor, shortening the DNAzyme (17E-2 and Sub_{Au}-2) has also been attempted. The decrease of bases on the DNAzyme resulted in the decrease of the affinity of the substrate and the enzyme strand. The new DNAzyme failed to assemble gold nanoparticles efficiently. Only a very small fraction of gold nanoparticles were in the aggregated forms. The isolated nanoparticle aggregates cannot re-assemble during the heating-and-cooling process. Therefore, this modification cannot be used in a sensor for Pb²⁺.

Effects of Nanoparticle Alignment on Nanoparticle Assembly and Pb²⁺ Sensing. We further investigated the effect of changing the alignment of the nanoparticles. The published design was based on the “head-to-tail” alignment of gold nanoparticles (Figure 4, inset a).²⁵ The use of the “head-to-tail” alignment is advantageous because it is easy to maintain stoichiometry. If the alignment is changed to the “tail-to-tail” alignment (Figure 4, inset b), gold nanoparticles functionalized with two different DNA have to be used (functionalized with 5'- and 3'-thiol-modified DNA, named DNA_{Au} and 3DNA_{Au}, respectively). The substrate is also changed to 35Sub_{Au} (Table 1). Surprisingly, if the nanoparticles were aligned in a “tail-to-tail” manner, the aggregates were insensitive to the presence of Pb²⁺ using the current detection method; the degree of aggregation was similar to that of the sample without Pb²⁺ added, even when up to 10 μM Pb²⁺ was added (Figure 4, empty squares). In contrast, most gold nanoparticles were in the separated state (Figure 4, solid circles) in the “head-to-tail” alignment when 4 μM Pb²⁺ was present. The UV-vis extinction spectra of the corresponding samples are provided in the Supporting Information. Because the change from “head-to-tail” alignment to the “tail-to-tail” alignment significantly decreases the steric hindrance during the assembly of gold nanoparticles, the rate for the DNAzyme to assemble nanoparticles in a “tail-to-tail” manner is much faster compared to that of the other alignment. Indeed, the color of the solution changes from red to purple as the temperature decreases to ~35 °C for the “tail-to-tail” alignment. However, to observe the color change for the “head-to-tail” alignment, the temperature has to be decreased to below 30 °C. Therefore, the “head-to-tail” alignment is the optimal alignment and this design will be used for the characterization of the DNAzyme-nanoparticle system.

Stoichiometry of the Substrate and the Enzyme Strand. Figure 1c shows the three components of the biosensor: the enzyme (17E), the substrate (Sub_{Au}), and nanoparticles (DNA_{Au}). They anneal to each other through DNA base-pairing interactions. The annealed products further cross-link to form blue nanoparticle aggregates. In the scheme, the enzyme strand and the substrate strand are drawn in such a manner that each substrate is annealed to one enzyme. This indicates that

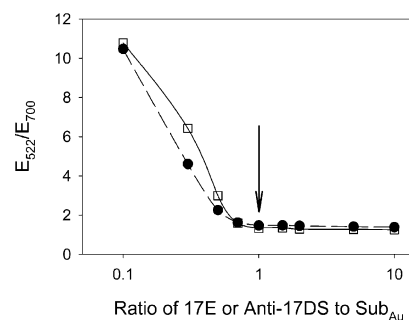


Figure 5. Ratio of 17E or Anti-17DS to Sub_{Au} is shown on the *x* axis. The degree of aggregation increases with more 17E or Anti-17DS added, until one equivalent was reached (indicated by a black arrow). Further increase of 17E or Anti-17DS did not increase the degree of aggregation further (lower extinction ratio indicates higher degree of aggregation.). This figure suggests that the ratio of 17E and Sub_{Au} in the nanoparticle aggregation is one to one.

the stoichiometry between the substrate and the enzyme strand is one to one. However, it is not evident that the enzyme strands must be present, because it is the substrate strand that acts as a linker. The presence of an enzyme strand appears to be optional. Different concentrations of the enzyme strand give different cleavage rates,^{27,28} and the detection and quantification of Pb²⁺ is based on the cleavage of the substrate strand by the enzyme. Therefore, control and optimization of the ratio of the substrate and enzyme are crucial for the high reproducibility of the sensor.

To determine the ratio of the substrate and enzyme in the aggregates, the following experiments were designed. To a series of samples with the same concentration of gold nanoparticles and substrate strand, different concentrations of the enzyme were added, ranging from 0 to 10 equivalents to the substrate. After aggregation, the extinction properties of the resulting aggregates were measured by UV-vis spectroscopy. The extinction ratios versus the amount of enzyme added are plotted in Figure 5.

The degree of aggregation increased with increasing amounts of the enzyme strand, up to one equivalent. Further increase of the enzyme strand did not cause additional increase in the degree of aggregation (Figure 5, solid circles). In the absence of the enzyme strand, no nanoparticle aggregates could be observed. This result gives strong support to the model that has been proposed in Figure 1c, in which the substrate and the enzyme strand are at a one-to-one ratio. If no enzyme strands are present, the aggregates cannot form. To identify the role of the enzyme strand in the process of nanoparticle aggregation, the enzyme (17E) was replaced by a 20-mer DNA (named Anti-17DS) that is totally complementary to 17DS (Figure 1a), and the same experiment was performed. Similar results were observed (Figure 5, empty squares), indicating that the enzyme strand and Anti-17DS have the same function in the formation of nanoparticle aggregates, which is to make the substrate (Sub_{Au}) backbone rigid by forming double-stranded DNA with the middle part of the substrate.

The explanation for the requirement of the presence of a DNA strand to make the substrate backbone rigid can be obtained after a detailed analysis of the aggregation process. When temperature slowly drops from above

the melting temperature of the system, an enzyme strand first anneals to a substrate strand. The annealing makes the center part of the substrate strand rigid, and can link gold nanoparticles on both ends because it has two "sticky ends" that are complementary to DNA on gold nanoparticles. If no enzyme strand is present, a substrate strand first anneals to a DNA strand on a gold nanoparticle using one of its "sticky ends". Because there is no DNA to make the substrate backbone rigid, the substrate strand could fold back and anneal to the other "sticky end" with another DNA strand on the same nanoparticle. Since the nanoparticle concentration is very low (~ 10 nM) and the local concentration of DNA is high (~ 160 DNA molecules have been shown to be on a 16-nm gold nanoparticle),⁴² the possibility for the substrate strand to find another nanoparticle is much smaller than to find a DNA strand on the same nanoparticle.

Control experiments further support the above explanation. If one base is deleted from each end of 17E (17E-2), and the substrate strand is accordingly shortened by two bases (Sub_{Au}-2), the stability of the shortened DNAzyme decreases. This shortened DNAzyme cannot assemble gold nanoparticles efficiently and the yield of nanoparticle aggregates is much lower compared to that of the original DNAzyme. If 17E and the substrate strand are extended, resulting in a DNAzyme with higher stability, the high efficiency of nanoparticle assembly is maintained. These results suggest that to have an efficient assembly of gold nanoparticles, the substrate strand should first anneal to a DNA strand that can make its backbone rigid before it anneals to DNA on gold nanoparticles.

This unique property of the system gives the intrinsic stoichiometry to the DNAzyme in the biosensor, which forms the basis for reproducible and quantitative detection. Different concentrations of the enzyme strand can be used to assemble nanoparticles. After separating and purifying the nanoparticle aggregates, the ratio of the substrate and enzyme in the aggregates is one to one, which ensures the high reproducibility of the sensor.

Effect of Temperature. The Pb²⁺ detection was performed by heating the sensor to above 50 °C, and subsequently cooling it slowly to room temperature. At 50 °C, gold nanoparticles, the substrate, and the enzyme are in the separated state because it is above the melting temperature of the DNA ($T_m = 46$ °C). The substrate cleavage occurs during the cooling process. Therefore, it is important to understand the temperature-dependent cleavage profile in the nanoparticle system, and to identify the temperature at which the cleavage is the most efficient. To this end, a sample of nanoparticle aggregates was heated to 60 °C and allowed to cool to a predetermined temperature, at which point Pb²⁺ was added to the sample. The temperature was kept constant at that temperature for 10 min to allow the Pb²⁺ induced cleavage reaction to occur. At the end of the 10 min, EDTA was added to chelate Pb²⁺ and thus stop the reaction. Then the sample was heated to 60 °C again and cooled slowly to room temperature. The degree of aggregation of the sample

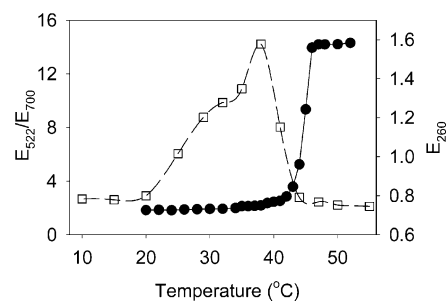


Figure 6. Relative ability of 17E to cleave the substrate strand during cooling of the melted gold nanoparticle aggregates (empty squares). No cleavage could be observed when the temperature was higher than 47 °C. The cleavage activity increased significantly from 44 to 37 °C and then began to drop. For comparison, the melting curve of gold nanoparticle aggregates assembled by the 17E and Sub_{Au} is also shown ($T_m = 46$ °C, solid circles). The extinction at 260 nm was monitored with increase of temperature (y -axis on the right side).

was monitored by UV-vis spectroscopy. A series of temperatures from 55 to 25 °C was tested, and the results are presented in Figure 6 (empty squares). The vertical axis on the left is the extinction ratio of the resulting nanoparticle aggregates. A higher ratio indicates a lower degree of aggregation, and thus a higher fraction of cleavage of the substrate strand in those 10 min. For comparison, the melting curve of the nanoparticle aggregates is also shown (Figure 6, solid circles). The vertical axis for the melting curve is the right axis of the plot. The extinction at 260 nm was monitored and the melting temperature was determined to be 46 °C under experimental conditions.

From Figure 6 (empty squares) it can be observed that at high temperatures (> 47 °C) almost no substrate is cleaved. As the temperature drops to below the melting temperature, the rate of cleavage increases significantly. The fraction of substrate cleaved reaches a maximum at ~ 37 °C, and then begins to drop. On the basis of the data presented in Figure 6, a microscopic process in the system as temperature decreases from 60 °C to room temperature can be deduced. At temperatures higher than the melting temperature of the system, the base-pairing interaction between DNA is smaller than the thermal energy and thus both the DNAzyme and nanoparticles are in the separated state. As temperature drops to below the melting temperature, the substrate and the enzyme strand can anneal. After annealing, the substrate can either be cleaved by the enzyme in the presence of Pb²⁺ or act as a linker to assemble gold nanoparticles. The substrate strands embedded into nanoparticle aggregates are protected from being cleaved. Therefore, there is a competition between the two processes. A higher Pb²⁺ concentration gives a larger fraction of cleavage, and the DNAzyme available to assemble nanoparticles is correspondingly decreased. The fraction of cleavage, and thus the degree of aggregation, is directly related to Pb²⁺ concentration and can be used for Pb²⁺ detection and quantification.

Effect of pH. A good sensor should be capable of performing detections in a wide pH range. Previous biochemical assays of the Pb²⁺-dependent "8-17" DNAzyme were carried out in the pH range from 4.8 to 6.5. This work indicated that a higher pH resulted in a faster cleavage rate.²⁸ In the current study, the pH range in which nanoparticles can be efficiently assembled by the

(42) Demers, L. M.; Mirkin, C. A.; Mucic, R. C.; Reynolds, R. A., III; Letsinger, R. L.; Elghanian, R.; Viswanadham, G. *Anal. Chem.* **2000**, *72*, 5535–5541.

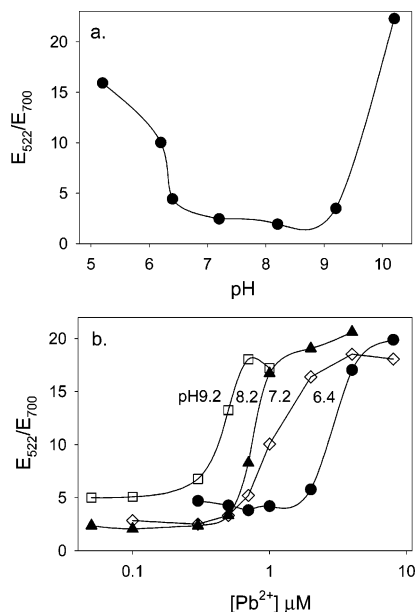


Figure 7. (a) Assembly of gold nanoparticles by the DNAzyme with different pH conditions in the absence of Pb^{2+} . (b) Pb^{2+} -dependent assembly of gold nanoparticles by the DNAzyme with different pH conditions. At each pH, the extinction ratio increases with increase of Pb^{2+} concentration, indicating decreased assembly.

DNAzyme was first tested. The pH-dependent assembly of nanoparticles is presented in Figure 7a. In the pH range of 6.4 to 9.2, nanoparticles can be efficiently assembled by the DNAzyme, because low extinction ratios were observed for these samples. For samples with pH values out of this range, the degree of aggregation decreased significantly, as can be observed from the increased extinction ratios. Because the formation of the aggregate relies on the base-pairing interaction of DNA, the strength of the base-pairing decreases at high pH because deprotonation of DNA bases prevents base-pairing.^{43,44} At pH 6.2, the sample without Pb^{2+} added gave an E_{522}/E_{700} ratio of ~ 10 (Figure 7a), indicating that the sensor is not sensitive at this pH. The lowest pH for the sensor to be useful was determined to be 6.4. Even at this pH, the extinction ratio was around 5 for the sample without Pb^{2+} added, as compared to an extinction ratio of around 2 for samples at pH 7–8. Therefore, the aggregation of gold nanoparticles is also affected at lower pH. DNA double helices are not expected to have reduced stability at pH 6.2 as compared to neutral pH. Thus, the stability of the DNA helix cannot be used to explain the decreased degree of aggregation. The reason for the decreased degree of aggregation at lower pH is unclear. One possibility is that this observation might be related to the stability of DNA-functionalized nanoparticles at lower pH.

Because the pH range for nanoparticles to aggregate efficiently was determined to be 6.4 to 9.2, the Pb^{2+} -dependent assembly of nanoparticles in this pH range was investigated and the results are presented in Figure 7b. The four curves in Figure 7b are the Pb^{2+} detection curves at pH 6.4, 7.2, 8.2, and 9.2, respectively. At each pH, a higher Pb^{2+} concentration gives a higher extinc-

tion ratio, indicating a larger fraction of cleavage and a lower degree of aggregation. If the Pb^{2+} -dependent aggregation at different pH values is compared, the trend that higher pH results in a faster cleavage rate for the DNAzyme is maintained up to pH 9.2. Considering the stability and the sensitivity of the sensor, the optimal pH for the detection should be in the range of pH 7.2 to pH 8.2, which is physiologically relevant. Samples with pH outside of the optimal range should be adjusted to this range.

Experimental Section

Oligonucleotides and Reagents. All oligonucleotides were purchased from Integrated DNA Technologies Inc. The two thiol-modified 12mer DNA were used as received after desalting by the company. All other oligonucleotides were purified by HPLC by the company. Gold nanoparticles with 13-nm diameter were prepared following literature procedures.¹⁰ The size of gold nanoparticles was verified by TEM (JEOL 2010). The 3'- and 5'-thiol-modified 12-mer DNA molecules were attached to gold nanoparticles using standard methods.¹⁰ The names and sequences of DNA used in the paper are listed in Table 1. The cleavage sites of the substrates are shown in boldface type (**ra**).

DNAzyme Activity Assay. The 17E enzyme (5 μM) and 500 nM 5'-TAMRA- (6-carboxytetramethylrhodamin) labeled substrate (Rh-17DS) were dissolved in 25 mM Tris acetate buffer, pH 7.2, with 300 mM NaCl in the presence or absence of 10 nM DNA_{Au}. The samples were annealed by heating to 90 °C and cooling to room temperature. To initiate the cleavage reaction, Pb^{2+} stock solution was added to make the final Pb^{2+} concentration 20 μM . Aliquots were taken out at different time points and the reactions were quenched by adding 90% formamide and 1 mM EDTA. The cleaved and uncleaved substrates were separated by 16% polyacrylamide gel electrophoresis. The percentage of cleavage was quantified using a Fuji FLA-3000 fluorescence image reader by exciting TAMRA at 532 nm. The experiments were run in duplicate to ensure the reproducibility of results.

Formation of Gold Nanoparticle Aggregates. In 25 mM Tris acetate buffer, pH 7.2, containing 300 mM NaCl, DNA_{Au}, Sub_{Au}, and 17E were dissolved to the final concentrations of 10, 170, and 340 nM, respectively. The mixture was incubated in a water-bath at 60 °C for 3 min and allowed to cool to room temperature over 2 h. Precipitate was observed. The tube was centrifuged for one minute and the supernatant was removed. The precipitate was washed with buffer and re-dispersed in the same buffer. This dispersion contained only aggregated gold nanoparticles and can be used as a sensor for Pb^{2+} detection. The formation of nanoparticle aggregation using different DNAzymes was performed using similar procedures by changing the DNAzyme only. For the formation of nanoparticle aggregation containing both 3'- and 5'-end thiol-modified DNA functionalized nanoparticles, 500 μL of each kind of nanoparticles were mixed. The concentration of DNAzyme and buffer were kept the same as those in the above preparations.

Melting Curves. Samples of nanoparticle aggregates assembled by DNAzymes were suspended in a buffer solution (25 mM Tris acetate buffer, pH 7.2, 300 mM NaCl) in a UV-vis sampling cell. The cell was capped to minimize water evaporation. A water-bath was used to control temperature. Before taking measurements at each temperature, the temperature was held constant for 2 min. The melting curves were obtained on a Hewlett-Packard 8453 spectrophotometer. The extinction at 260 nm was monitored with the increase of temperature.

Determination of the Ratio of 17E and Sub_{Au} in Nanoparticle Aggregates. Samples with 10 nM DNA_{Au}, 170 nM Sub_{Au}, and different 17E concentrations (from 0 to 1.7 μM) were prepared. The buffer was 300 mM NaCl and 25 mM Tris acetate (pH 7.2). The tubes were heated to 60 °C and cooled

(43) Izatt, R. M.; Christensen, J. J.; Rytting, J. H. *Chem. Rev.* **1971**, *71*, 439–482.

(44) Record, M. T., Jr. *Biopolymers* **1967**, *5*, 993–1008.

to room temperature over 2 h. The UV-vis extinction spectra of the resulting samples were taken to measure the degree of aggregation. The same experiment was repeated by replacing 17E with Anti-17DS. All UV-vis spectra were acquired on a Hewlett-Packard 8453 spectrometer.

Temperature-Dependent Cleavage Rate. An 80- μL portion of the 17E DNzyme-assembled nanoparticle aggregates (dispersed in 300 mM NaCl, 25 mM Tris acetate buffer, pH 7.2) was placed in a water-bath at 60 °C and incubated for 3 min. The color of the sensor turned from blue to red. The water-bath was turned off and the sample was allowed to cool to a chosen temperature, namely 55, 50, 47, 44, 41, 38, 35, 32, 29, 25, 20, 15, and 10 °C. Then 1.6 μL of 200 μM Pb^{2+} was added to the sample, giving a final Pb^{2+} concentration of ~ 4 μM . The sample was then placed back in the water-bath, and the temperature was adjusted to within ± 0.5 °C of the chosen temperature. After incubation for 10 min, 1.6 μL of 2 mM EDTA was added to stop the reaction, and the tube was taken out of the water-bath. The sample was again placed in a 60 °C water-bath for 3 min and then allowed to cool to room temperature over 2 h. The UV-vis spectrum of the resulting solution was measured.

Pb^{2+} Detection at Different pH Values. Buffers containing 300 mM NaCl at different pH values were prepared (pH 5.2 acetate buffer, pH 6.2, 6.4, MES, and pH 7.2 to 10.2 Tris acetate buffer). Nanoparticle aggregates were dispersed in these buffers (in the absence of Pb^{2+}) and were heated to 60 °C followed by a slow cooling to room temperature. Extinction spectra of the samples were then checked. On the basis of the results, Pb^{2+} -dependent studies were performed on samples at pH 6.4, 7.2, 8.2, and 9.2. Pb^{2+} (1 μL of stock solution) was added to 49 μL of nanoparticle aggregates dispersed in these buffers. The samples were heated and cooled slowly to room temperature over 2 h. Extinction spectra of the samples were checked to determine the aggregation states of the nanoparticles.

Conclusion

Incorporation of analyte-specific DNzymes into a DNA-functionalized gold nanoparticle system makes possible directed assembly of nanomaterials, with promising applications as biosensors. We found that the

presence of gold nanoparticles had no effect on the DNzyme activity and the presence of DNzyme has little effect on the melting properties of the DNA-functionalized nanoparticle aggregates, making it possible to optimize the nanoparticle assembly process and DNzyme activity independently. The DNzyme-assembled nanoparticle aggregates also have a sharp melting transition characteristic of cooperative behavior. A detailed characterization of the system showed that the optimal length of the DNzyme should be 9 base pairs on each end of the DNzyme, and the alignment of the DNA-functionalized gold nanoparticles should be "head-to-tail". In addition, the system possesses an intrinsic stoichiometry of 1:1 between the enzyme and substrate, which ensures its high reproducibility. The sensor works in a wide pH range (from 6.4 to 9.2), with the optimal performance near physiological pH (7.2–8.2). Finally, the optimal temperature of the system is 37 °C. We also found that the substrate DNA must have a rigid double-helical backbone before it can assemble nanoparticles efficiently. These findings allow optimization of the directed assembly process and thus make it possible to design highly sensitive and selective colorimetric biosensors.

Acknowledgment. This material is based upon work supported by the U.S. Department of Energy (NABIR program, DEFG02-01-ER63179), Nanoscale Science and Engineering Initiative of the National Science Foundation (DMR-0117792), and by the STC WaterCAMPWS of the National Science Foundation under agreement CTS-0120978.

Supporting Information Available: UV-vis extinction spectra of DNzyme-assembled nanoparticle aggregates in the presence of different Pb^{2+} concentrations (pdf). This material is available free of charge via the Internet at <http://pubs.acs.org>.

CM049453J